ACS OMEGA

http://pubs.acs.org/journal/acsodf

Article

Preparation and Characterization of Polycaprolactone (PCL) Antimicrobial Wound Dressing Loaded with Pomegranate Peel Extract

Yize Wang, Xianzhu Wang, Dan Zhou, Xin Xia, Huimin Zhou, Ying Wang,* and Huizhen Ke*

Cite This: *ACS Omega* 2023, 8, 20323−20331

Read Online

ACCESS | Metrics & More | Article Recommendations

ABSTRACT: In recent years, medicinal plant extracts have received remarkable attention due to their wound-healing properties. In this study, polycaprolactone (PCL) electrospun nanofiber membranes incorporated with different concentrations of pomegranate peel extract (PPE) were prepared. The results of the SEM and FTIR experiments demonstrated that the morphology of nanofiber is smooth, fine, and bead-free, and the PPE was well introduced into the nanofiber membranes. Moreover, the outcomes of the mechanical property tests demonstrated that the nanofiber membrane made of PCL and loaded with PPE exhibited remarkable mechanical characteristics, indicating that it could fulfill the essential mechanical requisites for wound dressings. The findings of the in vitro drug release investigations indicated that PPE was instantly released within 20 h and subsequently released gradually over an extended period by the composite nanofiber membranes. Meanwhile, the DPPH radical scavenging test confirmed that the nanofiber membranes loaded with PPE exhibited significant antioxidant properties. Antimicrobial experiments showed higher PPE loading, and the nanofiber membranes showed higher antimicrobial activity against *Staphylococcus aureus*, *Escherichia coli*, and *Candida albicans*. The results of the cellular experiments showed that the composite nanofiber membranes were nontoxic and promoted the proliferation of L929 cells. In summary, electrospun nanofiber membranes loaded with PPE can be used as a wound dressing.

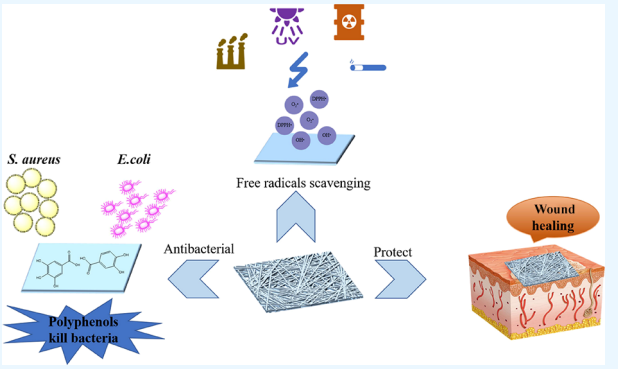

1. INTRODUCTION

Skin, the largest organ of the human body, regulates metabolism and maintains homeostasis.[1] Furthermore, skin is crucial in protecting the body against microorganism invasion and harmful environmental factors.[2] In the case of any impairment in the morphology or function of the skin, it is imperative to promptly apply a dressing that serves as a barrier to the affected wound area.[3] However, traditional wound dressing, including gauze, bandages, and others, cannot meet the diverse needs of patients nowadays.[4] Therefore, it is crucial to formulate a wound dressing that can effectively meet the diverse requirements of patients. A desirable dressing must have the capability to quickly absorb wound exudates, maintain the appropriate moisture level in the wound area, enable gas exchange, and isolate microorganisms.[5,6] Furthermore, the wound dressing should also possess biocompatibility,[7] antimicrobial,[8] anti-inflammatory,[9] and antioxidant[10] properties.

Nanofibrous membranes for wound dressing manufactured by electrospinning have attracted considerable attention in recent years.[11] The nanofibrous membranes have a high surface-to-volume ratio which could mimic the extracellular matrix (ECM) of the targeted site, facilitating cell adhesion and proliferation.[12] Extremely fine pore size might isolate the bacterium from the wound area, and high porosity promotes gas exchange and absorption of excess exudate.[13] Furthermore, using electrospinning, the wound dressing could be customized based on the needs of patients.[14] Electrospinning is deemed as a promising technique for manufacturing wound dressings. Several materials have been utilized in recent times to create electrospun materials. One such material is polycaprolactone (PCL), which is a polymer with remarkable biodegradability, biocompatibility, electrospinnability, and mechanical robustness. The FDA has approved the use of PCL for biomedical applications.[15] Hence, PCL could be an excellent material for manufacturing electrospun nanofiber membranes.

Received: December 25, 2022
Accepted: May 10, 2023
Published: May 26, 2023

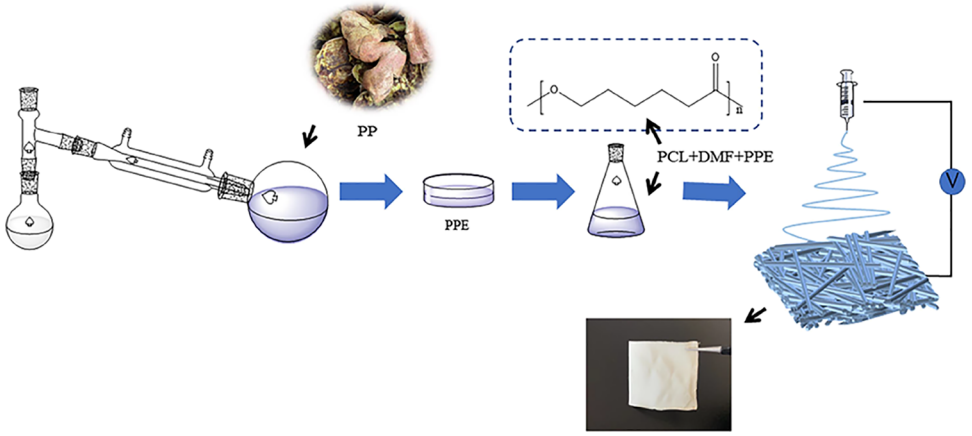

Figure 1. Preparation of electrospun nanofiber membranes loaded with PPE.

Many bioactive or antibacterial agents were incorporated into the electrospun nanofiber membranes to improve the wound-healing effects.[16−18] From ancient times, some plant extracts that are rich in biologically active substances, including flavonoids, phenols, polysaccharides, etc., with antimicrobial, anti-inflammatory, and antioxidant properties have been used to accelerate wound healing.[19−21] *Punica granatum* L., a fruit native to the Balkans, Iran, and neighboring countries, is widely cultivated in Xinjiang, Henan, Jiangsu, and other parts of China. Pomegranate peel is an excellent source of polyphenols with potential antibacterial, antifungal, anti-inflammatory, antioxidant, antiparasitic, and anticancer properties.[22−25] According to Aminlari and co-workers,[26] PPE could promote wound healing by increasing FN1 gene expression and extracellular matrix components such as GAGs and collagen content and hence can be considered a therapeutic agent for wound healing. To date, no studies on electrospun nanofiber membrane-incorporated PPE for wound dressing application have been reported.

The present investigation aims to produce PCL/PPE nanofiber membranes using electrospinning due to their exceptional wound-healing properties. The nanofiber membranes will be evaluated for their morphology, chemical structure, hydrophilic nature, release kinetics, and mechanical characteristics. Moreover, the antioxidant activity, antimicrobial activity, biocompatibility, and in vitro wound-healing efficiency were also analyzed.

2. MATERIALS AND METHODS

2.1. Materials. Pomegranate peels were collected in Urumqi, Xinjiang. Folin phenol reagent (BR 1 mol/L, LOT: S25N11J131971) and gallic acid standard (B20851 −20 mg, CAS#140-91-7, HPLC ≥98%) were purchased from Shanghai Yuanye Biotechnology Co., Ltd., Polycaprolactone (PCL) (M_w = 80,000) was provided by Shanghai FanTai Biotechnology Co., Ltd., NN-Dimethylformamide (DMF), Alkaline Phosphate (PBS, PH7.4), 1-Diphenyl-2 -Trinitrophenylhydrazine (DPPH), and other chemical reagents were all analytical pure.

2.1.1. Preparation of Pomegranate Peel Extracts. Pomegranate peels were collected and washed twice with deionized water to remove impurities. The pomegranate peels were then dried in a cool place and ground into powder using a pulverizer. After sieving through 40 mesh, 100 g of the powder was soaked in 600 mL of 70% (v/v) ethanol for 4 h at 60 °C. The solution was filtered via filter paper and concentrated using a rotary evaporator at 60 °C. The pomegranate peel extracts (PPEs) were collected and stored at 4 °C for subsequent use. Finally, the polyphenol content in PPE was determined by Folin−Ciocalteu method.

2.1.2. Preparation of PCL and PCL/PPE Electrospinning Nanofibers. Initially, a PCL solution (20%, w/v) was obtained by dissolving PCL in DMF. Subsequently, varying amounts of PPE (5, 7.5, 10% w/w of PCL) were dissolved in the PCL solution. The electrospinning conditions were set as follows: 18 cm distance between the needle and the collector, 21 kV voltage, and 0.5 mL/h flow rate. Figure 1 depicts the preparation process. The PPE nanofiber membranes with different contents (5, 7.5, 10% w/w of PCL) were named PCL/5PPE, PCL/7.5PPE, and PCL/10PPE, respectively.

2.1.3. Scanning Electron Microscope (SEM) Analysis. The morphology of the nanofiber membranes was examined by SEM. Electrospun nanofibrous membranes were mounted onto the aluminum foil and coated with gold palladium. The images obtained from SEM were captured, and the mean diameters of fibers were calculated using Image plus computer software.

2.1.4. Fourier-Transform Infrared Spectroscopy (FTIR) Analysis. The interaction between the molecules of the polymer and the functional groups of PPE was investigated using FTIR. FTIR spectra were recorded in the range of 4500−500 cm^{-1} at 4 cm^{-1} resolution.

2.1.5. Water Contact Angle. The hydrophilic properties of the nanofiber membranes were assessed using the water contact angles measurement (DCAT21, Dataphysics Instrument GmbH, Germany). The nanofiber membranes were sliced into squares (3 × 3 cm^2), and 5 μL of deionized water droplets were dispersed on their surface. The contact angles of different nanofiber membranes were then examined and recorded using the equipment software.

2.1.6. Determination of Mechanical Properties. The mechanical properties such as tensile strength, breaking strength, and Young's modulus of nanofiber membranes were examined using a fiber tensile tester. Rectangular pieces (3 × 0.5 cm^2) of the nanofiber membranes were cut and clamped onto the machine jaws. The tests were conducted at a stretching rate of 10 mm/min, and the resulting data were recorded.

2.1.7. In Vitro Drug Release Capability. The nanofiber membranes were sliced into rectangular pieces (4 × 5 cm^2), and 25 mg of each sample was immersed in 6 mL of phosphate buffer solution (PBS, PH7.4). The samples were then placed in

https://doi.org/10.1021/acsomega.2c08180
ACS Omega 2023, 8, 20323−20331

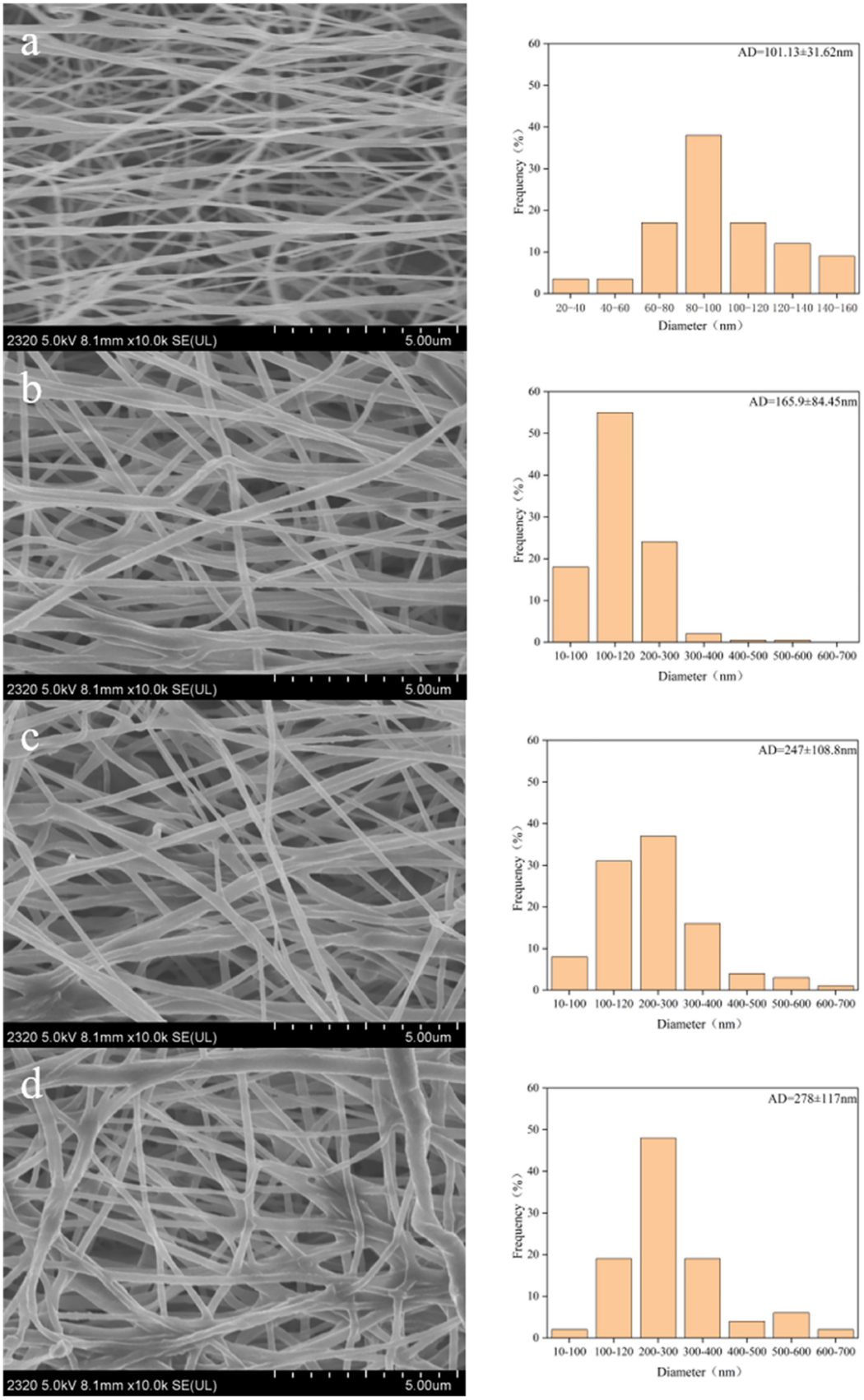

Figure 2. SEM images and histograms for the size distribution of wound dressing: (a) PCL, (b) PCL/5PPE, (c) PCL/7.5PPE, and (d) PCL/10PPE.

https://doi.org/10.1021/acsomega.2c08180
ACS Omega 2023, 8, 20323−20331

a shaker and agitated at 100 rpm for 60 h at 37 °C. At each time point, 3 mL of PBS solution was removed and replaced with an equal amount of fresh PBS. The PBS solution was examined at a wavelength of 765 nm, and the percentage of PPE released from nanofibers was calculated using the calibration plot.

2.1.8. Antioxidant Activity. The antioxidant property of the composite nanofiber membranes was determined using the DPPH method.[27] A DPPH ethanol solution (0.2 mg/mL) was prepared and kept in the dark. The nanofiber membrane samples were prepared as follows: 25 mg of PCL, PCL/5PPE, PCL/7.5PPE, and PCL/10PPE nanofiber membranes were weighed and then sliced into small pieces. These membrane pieces were soaked in 3 mL of absolute ethanol. After 5 h, 2 mL of the supernatant was mixed with 2 mL of the DPPH solution and stored in the dark for 30 min. The OD value of the solution was detected using an ultraviolet spectrophotometer at 517 nm. The antioxidant activity was calculated according to the following equation (eq 1):

$$E(\%) = \left[1 - \frac{A_i - A_j}{A_o}\right] \times 100\% \quad (1)$$

where A_o is the absorbance of the control at 517 nm; A_j is the absorbance of the blank at 517 nm; A_i is the absorbance of the sample at 517 nm.

2.1.9. In Vitro Antimicrobial Activity. The disc diffusion method was used to detect the antimicrobial activity of composite nanofiber membranes against *Staphylococcus aureus*, *Escherichia coli*, and *Candida albicans*. At first, the nanofiber membranes were sliced into pieces (1 × 1 cm^2). After undergoing UV sterilization, the nanofiber membranes were arranged on plates coated with *S. aureus*, *E. coli*, and *C. albicans*, correspondingly. These plates were then incubated (plates with *S. aureus* and *E. coli* were incubated at 37 °C, whereas plates with *C. albicans* were incubated at 28 °C). After 24 h, the diameter of the inhibition zones was observed and recorded. The experiment was repeated thrice.

2.1.10. Cytotoxicity Assay. The cytotoxicity of the nanofiber membranes was determined using the CCK8 assay in mouse fibroblast (L929) cells. At first, both sides of the nanofiber membranes were sterilized under UV irradiation for 30 min. The membranes were then immersed in a DMEM medium containing 10% fetal bovine serum, 100 U/mL penicillin, and 1% streptomycin for 24 h. The L929 cells were seeded at 96 well plates (1 × 10^4 cells/well) and incubated at 37 °C for 24 h. The medium in 96 well plates was then replaced with extract medium. The plates were kept further in an incubator for 24 to 48 h. Subsequently, 10 μL of CCK8 was introduced into each well, and the plates were incubated for 3 h. The absorbance value of each sample (n = 3) was measured at 450 nm after incubation. The cell viability was calculated as follows (eq 2):

$$\text{Cell viability } (\%) = \frac{A_{sample}}{A_{control}} \times 100\% \quad (2)$$

where A_{sample} and $A_{control}$ represent the absorption value of the medium soaked with or without nanofiber membranes, respectively.

2.1.11. In Vitro Cell Migration Assay. The in vitro wound-healing effects of the composite nanofiber membranes were obtained using the scratch assay. L929 (1 × 10^5 cells/well) cells were seeded in a 24 well plate and incubated at 37 °C for 24 h. A scratch was created using a 200 μL micropipette tip, and the sterile composite nanofiber membranes (1 mg/well) were added to the scratch. The 24 well plates were then kept in an incubator at 37 °C for another 24 h. The scratches were photographed using a light microscope at 0 and 24 h to capture the changes. The cell migration rate was analyzed using the Image plus computer software and calculated as follows (eq 3):

$$\text{Cell migration rate } (\%) = \frac{(Wd^0 - Wd^t)}{Wd^0} \times 100 \quad (3)$$

where Wd^0 is the distance between the scratch boundaries at 0 h, and Wd^t is the distance between the scratch boundaries at the designated time.

2.2. Statistical Analysis. All data are the average of three replications and are expressed as mean ± SEM. One-way ANOVA was used to determine the statistical significance, and the data and images were processed using Origin 2021 and Graph Pad Prism 5 software.

3. RESULTS AND DISCUSSION

3.1. Determination of Polyphenol Content in PPE. PPE consists of a variety of complex and diverse bioactive constituents, with polyphenols being the primary components. The polyphenols present in PPE exhibit both antibacterial and antioxidant properties. Therefore, we employed the Folin−Ciocalteu method to evaluate the polyphenol content in PPE. The results showed that the content of polyphenols in PPE was 135.30 mg/g. Skrt et al.[28] also used the ethanol solvent extraction method to extract polyphenols in pomegranate peel, and the yield of extracted polyphenols was 30.5 mg/g after optimizing the extraction conditions. This value was lower than the amount of extracted polyphenols in this study. This variation may be due to the extraction conditions and the solvent used, and may also be due to the difference with variation related to the differences in the geographical area of origin resulted.[29]

3.2. Morphology and Diameter Distribution of Nanofibers. The SEM was utilized to analyze the morphology of the nanofiber membranes, which contained different concentrations of PPE. Figure 2a−d corresponds to the SEM images of PCL, PCL/5PPE, PCL/7.5PPE, and PCL/10PPE, respectively. The nanofibers exhibited a smooth, fine, and bead-free structure. The incorporation of the PPE increases the mean diameter of the nanofibers from 101.13 ± 31.62 to 278 ± 117 nm. This could be attributed to the PPE increasing the viscosity of the spinning solution and decreasing the conductivity of the solution.[30]

3.3. FTIR Analysis. In this study, FTIR spectroscopy was used to verify the encapsulation of PPE in PCL. Figure 3 depicts the absorption peaks of PCL, PCL/5PPE, PCL/7.5PPE, and PCL/10PPE. In the case of PCL, a peak at 1733 cm^{-1} attributes to the C═O stretching.[31] In the case of PCL, the peaks at 1733 and 1260 cm^{-1} are attributed to C═O and C−O−C stretching vibrations, and the absorption peaks at 2954 and 2874 cm^{-1} are caused by asymmetric stretching vibrations of $-CH_2$, all of which are characteristic peaks of PCL.[32−35] Incorporating PPE into PCL results in a slight reduction in the intensity of the peaks compared to pure PCL. One of the major peaks of PPE, located at 3352 cm^{-1}, corresponds to the −OH vibration of polyphenols in PPE. As the concentration of PPE increases, this peak becomes

https://doi.org/10.1021/acsomega.2c08180
ACS Omega 2023, 8, 20323−20331

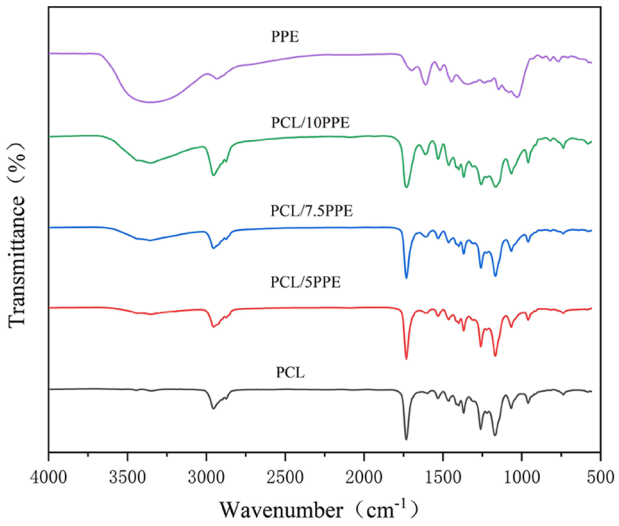

Figure 3. FTIR spectra of nanofiber membranes.

broader.[36] In the composite nanofiber membrane, the characteristic peak of PCL is slightly shifted due to the formation of hydrogen bonds between the hydroxyl group in the polyphenol and the carbonyl group in the PCL. This leads to an averaging of the density of the carbonyl electron cloud.[37] FTIR spectra confirmed that PPE is successfully incorporated into the nanofibers.

3.4. Water Contact Angle. The hydrophilic nature of the wound dressing facilitates the absorption of wound exudate and accelerates wound healing.[38] On nanofiber membranes, a hydrophilic surface could stimulate cell adhesion, spreading, and proliferation on nanofibers membranes. The water contact angle is commonly used to assess the hydrophilicity of a material. A contact angle of 0−90° generally indicates good hydrophilicity, whereas a contact angle of 90−180° indicates good hydrophobicity.[39] In this study, the dynamic water contact angle measurement was performed to investigate the effect of PPE on surface wettability (Figure 4). The contact angle of pure PCL remains constant at 134.4 ± 2.00°. However, when the PPE content of the nanofiber membranes increases, the water contact angle at 10 s decreases from 49.47 ± 2.18° (PCL/5PPE) to 21.93 ± 0.25° (PCL/10PPE). The PPE content has a negative relationship with the water contact angle value. This may be attributed to a large amount of

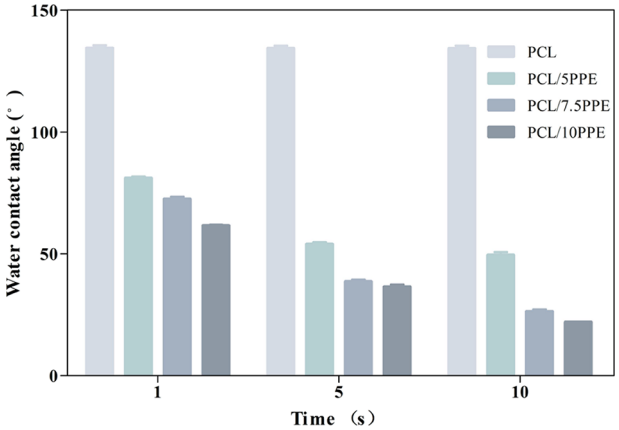

Figure 4. Water contact angle of nanofiber membranes at 1, 5, and 10 s, respectively.

hydrophilic substances, such as polyphenols, which existed in PPE.[40]

3.5. Mechanical Properties. An ideal wound dressing should have adequate strength and elasticity to that of the skin. The breaking strength, elongation at break, and Young's modulus of PCL, PCL/5PPE, PCL/7.5PPE, and PCL/10PPE are shown in Table 1. The break strength, elongation at break,

Table 1. Mechanical Properties of Nanofiber Membranes

	breaking strength (MPa)	elongation at break (%)	Young's modulus (MPa)
PCL	2.75 ± 0.04	38.51 ± 3.05	7.13 ± 0.10
PCL/5PPE	8.21 ± 1.27	132.48 ± 12.06	6.2 ± 0.96
PCL/7.5PPE	10.43 ± 2.09	124.24 ± 21.00	8.39 ± 1.68
PCL/10PPE	11.47 ± 1.20	65.85 ± 6.75	17.42 ± 1.82

and Young's modulus of pure PCL are 2.75 ± 0.04 MPa, 38.51 ± 3.05%, and 7.13 ± 0.10 MPa, respectively, while compared to pure PCL, incorporation of the PPE increases the tensile strength and Young's modulus. The break strength, elongation at break, and Young's modulus of the PCL/10PPE nanofiber membrane are 11.47 ± 1.20 MPa, 65.85 ± 6.75%, and 17.42 ± 1.82 MPa. One reason might be that the phenolic hydroxyl groups of polyphenols in PPE react with the carbonyl oxygen atoms in PCL to form hydrogen bonds, enhancing their mechanical properties. Another reason might be that the polyphenols contain aromatic structures, which can increase the mechanical properties of the membrane.[41,42]

3.6. In Vitro Drug Release Capability. Nanofiber membranes are used as a carrier for the delivery of PPE. While polyphenols, being the major component of PPE, play a key role in antimicrobial and antioxidant activities.[43] Therefore, the release of polyphenols is depicted as the release profile of PPE. Figure 5 depicts the release process, which may be

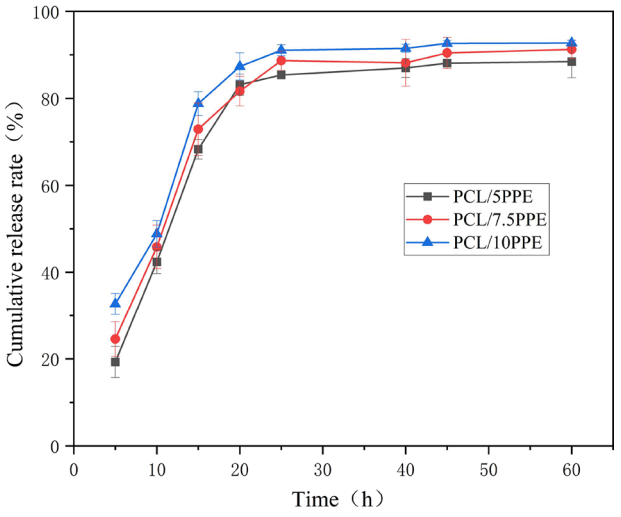

Figure 5. Cumulative release profile of nanofiber membranes within 60 h.

divided into two stages.[44] In the initial stage, a burst release of PPE is observed within 20 h after the nanofiber membranes were soaked in PBS. The PPE releases from PCL/5PPE, PCL/7.5PPE, and PCL/10PPE were 88.46 ± 3.75, 91.24 ± 2.10, and 92.72 ± 0.61%, respectively (Figure 6). The hydrophilic groups in the polyphenols and the large number of extracts

https://doi.org/10.1021/acsomega.2c08180
ACS Omega 2023, 8, 20323−20331

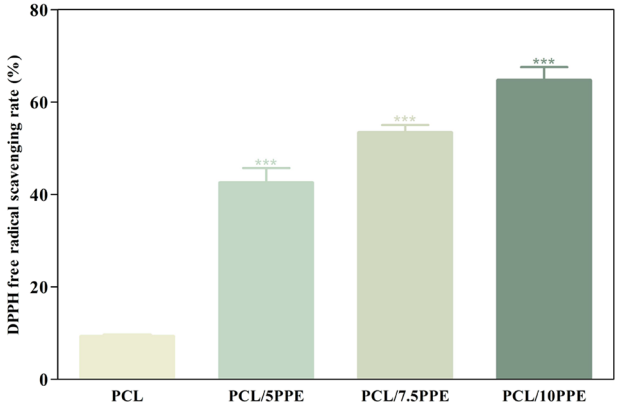

Figure 6. Antioxidant activity of nanofiber membranes, respectively. Data are presented as mean ± SEM (n = 3). The significant difference is marked by three asterisks (***) for P < 0.001 PCL/PPE vs PCL.

dispersed in the nanofibers may be strongly associated with the burst release. Then, the sustained release from nanofiber membranes is shown from 20 to 60 h. This could be attributed to the continued release of PPE in nanofiber. Furthermore, the concentration of PPE increases the release of PPE.

3.7. Antioxidant Activity. Free radicals accumulated in the wound site can cause inflammation and delay wound healing. Wound dressings should have certain antioxidant properties to resist the damage caused by the accumulation of excessive free radicals.[45] Studies have demonstrated that polyphenols in PPE possess remarkable antioxidant activity and are capable of eliminating free radicals.[46] To evaluate the antioxidant activity of the nanofiber membranes, the DPPH assay was employed. The results, depicted in Figure 6, indicate that the scavenging ability of pure PCL is significantly lower compared to the other groups. Specifically, the scavenging rate of PCL is 9.27 ± 0.28%. In contrast, the incorporation of PPE increases the scavenging rate of the composite nanofiber membranes from 42.51 ± 3.21 to 64.67 ± 2.88%. The difference in antioxidant activity between the PCL and PPE-loaded nanofiber membranes is statistically significant. PPE incorporation significantly improves the antioxidant activity of membranes. The antioxidant strength of PPE is determined by the number of phenolic hydroxyl groups present in its polyphenol molecules, resulting in a higher proton-donating capacity that stabilizes DPPH radicals.[47] Consequently, a higher PPE content in the nanofiber membrane corresponds to an increased polyphenol content and DPPH radical scavenging rate. Therefore, incorporating PPE into nanofiber membranes has the potential to enhance the antioxidant capabilities of wound dressings.

3.8. Antimicrobial Activity. Microbiological contamination was a major cause of delay in wound healing.[48] Therefore, an ideal wound dressing should have to contain antimicrobial properties. However, in recent years, there has been an increase in the use of antibiotics with many side effects on patients, leading to the rise of superbug.[49] PPE, being a natural extract from plant peel, would have lower side effects and could prevent microbial growth.[50] In clinical studies, the most prevalent organisms observed to cause wound infection were *E. coli*, *S. aureus*, and *C. albicans*.[51,52] A disc diffusion assay was performed to evaluate the nanofiber membranes' antimicrobial properties. The results, presented in Figure 7 and Table 2,

Table 2. Diameter of the Inhibition Zone of Nanofiber Membranes

	diameters of the inhibitory zone (mm)		
sample	*E. coli*	*S. aureus*	*C. albicans*
PCL	0	0	0
PCL/5PPE	13.27 ± 0.70	16.61 ± 0.17	11.67 ± 0.30
PCL/7.5PPE	15.73 ± 0.16	18.73 ± 0.17	17.67 ± 0.28
PCL/10PPE	19.15 ± 0.76	22.81 ± 0.29	20.01 ± 0.36

demonstrate that pure PCL lacks antimicrobial activity. However, as the concentration of PPE in the nanofiber membranes increases, the antimicrobial activity against *E. coli*, *S. aureus*, and *C. albicans* is enhanced. Moreover, the PCL/PPE nanofiber membranes exhibit superior antimicrobial activity against *E. coli*, *S. aureus*, and *C. albicans* in comparison to pure PCL. The diameter of the inhibition zone of PCL/10PPE against *E. coli*, *S. aureus*, and *C. albicans* reaches 19.15 ± 0.76, 22.81 ± 0.29, and 20.01 ± 0.36 mm, respectively. This conclusion could be explained by the fact that high polyphenol levels hinder the formation of microbial biofilms, hence decreasing their growth and reproduction.[53] The antimicrobial activity of PPE nanofibers against *S. aureus* is superior to that of *E. coli*. Wang et al.[54] suggested that this may be due to differences in the cell membrane structure of *S. aureus* and *E. coli*. Compared to *S. aureus*, *E. coli* has an additional phospholipid outer membrane that acts as a barrier to PPE. In this study, the successful introduction of PPE results in nanofiber membranes with good antibacterial properties.

3.9. Cytotoxicity Analysis. Fibroblasts are the major cells of the dermis, which play a critical role in the reconstruction of

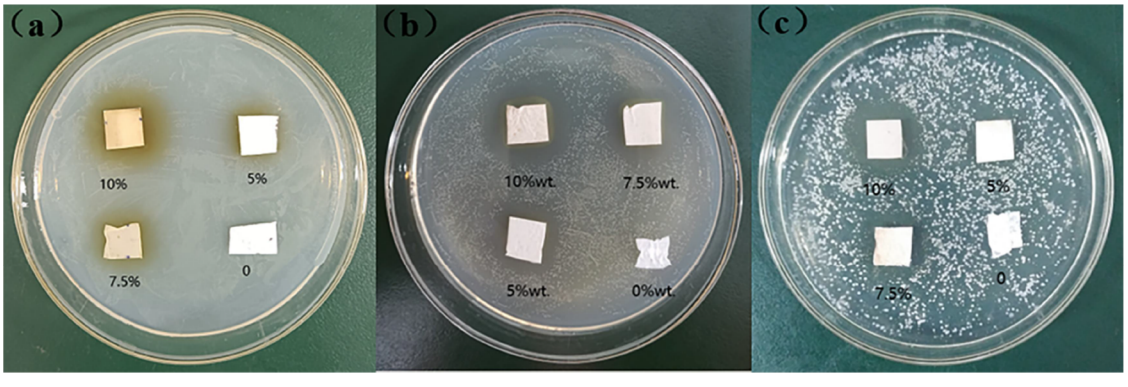

Figure 7. Antimicrobial activity of PCL and PCL/PPE nanofiber membranes. (a) *E. coli*, (b) *S. aureus*, and (c) *C. albicans*.

https://doi.org/10.1021/acsomega.2c08180
ACS Omega 2023, 8, 20323−20331

the tissue; hence, the L929 cell line is used in this test.[55] To assess the cytotoxicity of the nanofiber membranes containing varying concentrations of PPE, the CCK8 assay was conducted. The results, depicted in Figure 8, indicate that

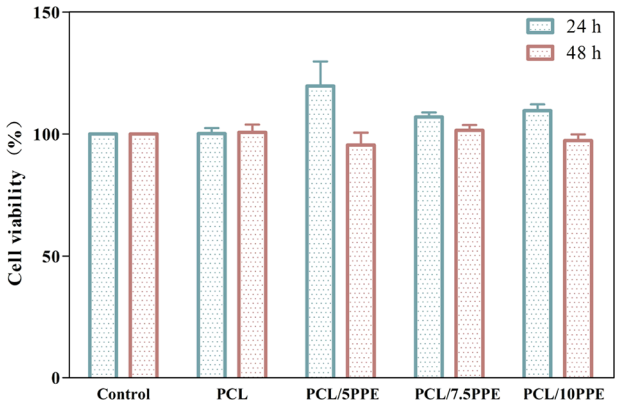

Figure 8. Cell viability of L929 cultured in the leach of nanofiber membranes incorporated with different concentrations of PPE at 24 and 48 h.

the viability of cells is not affected by exposure to the leachate medium of the nanofiber membranes. The cell viability of nanofiber membranes ranges from 100.1 ± 2.00 to 119.7 ± 4.45% at 24 h and then from 95.5 ± 2.00 to 101.5 ± 3.6% after 48 h (control was 100%). These results confirm that the nanofiber membranes exhibit good biocompatibility, and PPE could promote cell proliferation.[56]

3.10. In Vitro Wound-Healing Assay. Cell migration induces wound contraction during wound healing, which is an important step in triggering later stages of healing.[57] The cell migration effect of PCL/PPE nanofibrous membranes was assessed in this study using a cell scratch experiment, as depicted in Figures 9 and 10. The results demonstrate that the cell migration rates of the blank and PCL groups were 45.39 ± 1.46 and 50.72 ± 1.38%, respectively. However, the cell migration rates of the PCL/5PPE, PCL/7.5PPE, and PCL/10PPE groups were significantly higher, measuring 70.68 ± 0.94, 69.97 ± 1.16, and 84.92 ± 0.73%, respectively. The results reveal that the electrospun membrane with PPE significantly promoted the migration of L929 cells. Therefore, PPE-loaded electrospun nanofibrous membranes have the potential to promote skin wound healing.

4. CONCLUSIONS

In this study, PCL loaded with varying amounts of PPE is successfully manufactured using the electrospun method for wound dressing preparation. The morphology, physiomechanical, and biological properties of the membranes were all investigated. According to the SEM assay, the morphology of the nanofiber is uniform and bead-free. FTIR analyses confirm that the PPE is successfully incorporated into the nanofibers. With the increasing content of the PPE, the mechanical properties, hydrophilic properties, and oxidation resistance of the membranes are improved. The in vitro release kinetics of PPE indicates that it is initially released in bursts for the first 20 h, followed by a sustained release for the subsequent 40 h. The presence of PPE enhances the antimicrobial properties of the membranes against *E. coli*, *S. aureus*, and *C. albicans*. Additionally, the results of the CCK8 assay and scratch assay suggest that incorporating PPE improves the biocompatibility

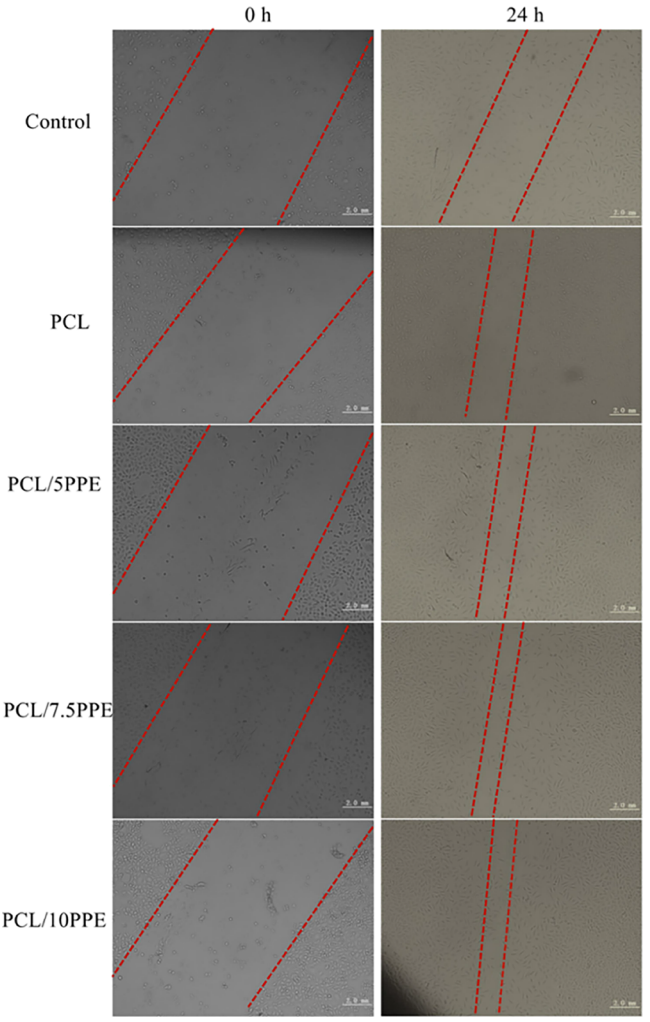

Figure 9. Morphology of L929 cells cultured at 0 and 24 h of control, PCL, PCL/5PPE, PCL/7.5PPE, and PCL/10PPE.

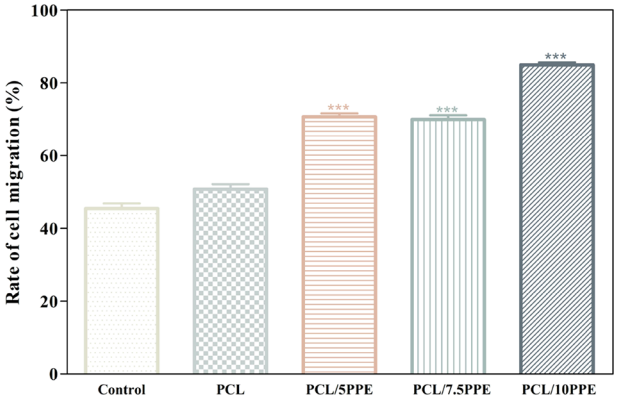

Figure 10. Rate of cell migration of nanofibers membranes in vitro. Data are presented as mean ± SEM (n = 40). The significant difference is marked by three asterisks (***) $P < 0.001$ PCL/PPE vs Control and PCL.

of the membranes and promotes the proliferation of L929 cells. Based on the findings, composite nanofiber membranes combined with PPE could be a promising candidate for wound dressings.

https://doi.org/10.1021/acsomega.2c08180
ACS Omega 2023, 8, 20323−20331

AUTHOR INFORMATION

Corresponding Authors

Ying Wang − *College of Textile and Clothing, XinJiang University, Wulumuqi 830046, China*; orcid.org/0000-0002-3404-8884; Email: xjuwangying@126.com

Huizhen Ke − *College of Fashion and Art Engineering, Minjiang University, Fuzhou, Fujian 350108, China*; Email: kehuizhen2013@163.com

Authors

Yize Wang − *College of Textile and Clothing, XinJiang University, Wulumuqi 830046, China*

Xianzhu Wang − *College of Textile and Clothing, XinJiang University, Wulumuqi 830046, China*

Dan Zhou − *College of Textile and Clothing, XinJiang University, Wulumuqi 830046, China*

Xin Xia − *College of Textile and Clothing, XinJiang University, Wulumuqi 830046, China*

Huimin Zhou − *College of Textile and Clothing, XinJiang University, Wulumuqi 830046, China*

Complete contact information is available at: https://pubs.acs.org/10.1021/acsomega.2c08180

Author Contributions

Y.W. and X.W. contributed equally to this work and should be regarded as co-first authors. Y.W.: methodology, software, and writing - review and editing. X.W.: study design, data curation, Photo shooting, data curation, writing - original draft. D.Z.: methodology and software. X.X.: formal analysis, methodology, supervision. H.Z.: formal analysis, methodology, supervision. Y.W.: conceptualization, funding acquisition resources, and writing − review and editing. H.K.: funding acquisition, resources, and writing − review and editing.

Notes

The authors declare no competing financial interest.

ACKNOWLEDGMENTS

This research was supported by The General Program of Xinjiang Natural Science Foundation (2021D01C059); The Xinjiang University Scientific Research Fund of Doctor (2019720001); The Open Project Program of Fujian Key Laboratory of Novel Functional Textile Fibers and Materials, Minjiang University China (FKLTFM21XX); Innovative training program of college students (202110755024).

REFERENCES

(1) Kruse, V.; Neess, D.; FæRgeman, N. J. The Significance of Epidermal Lipid Metabolism in Whole-Body Physiology. *Trends Endocrinol. Metab.* **2017**, *28*, 669−683.

(2) Skowron, K.; Bauza-Kaszewska, J.; Kraszewska, Z.; Wiktorczyk-Kapischke, N.; Grudlewska-Buda, K.; Kwiecinska-Pirog, J.; Walecka-Zacharska, E.; Radtke, L.; Gospodarek-Komkowska, E. Human Skin Microbiome: Impact of Intrinsic and Extrinsic Factors on Skin Microbiota. *Microorganisms* **2021**, *9*, 543.

(3) Gushiken, L. F. S.; Beserra, F. P.; Bastos, J. K.; Jackson, C. J.; Pellizzon, C. H. Cutaneous Wound Healing: An Update from Physiopathology to Current Therapies. *Life* **2021**, *11*, 665.

(4) Coco Ning, C.; Logsetty, S.; Ghughare, S.; Liu, S. Effect of hydrogel grafting, water and surfactant wetting on the adherence of PET wound dressings. *Burns* **2014**, *40*, 1164−1171.

(5) Li, X. M.; Wang, C.; Yang, S.; Liu, P.; Zhang, B. Electrospun PCL/mupirocin and chitosan/lidocaine hydrochloride multifunctional double layer nanofibrous scaffolds for wound dressing applications. *Int. J. Nanomedicine* **2018**, *13*, 5287−5299.

(6) Mazor, E.; Zilberman, M. Effect of gamma-irradiation sterilization on the physical and mechanical properties of a hybrid wound dressing. *Polym. Adv. Technol.* **2017**, *28*, 41−52.

(7) Lai, W.-F.; Hu, C.; Deng, G.; Lui, K.-H.; Wang, X.; Tsoi, T.-H.; Wang, S.; Wong, W.-T. A biocompatible and easy-to-make polyelectrolyte dressing with tunable drug delivery properties for wound care. *Int. J. Pharm.* **2019**, *566*, 101−110.

(8) Viswanathan, K.; Babu, D. B.; Jayakumar, G.; Raj, G. D. Antimicrobial and skin wound dressing application of molecular iodine nanoparticles. *Mater. Res. Express* **2017**, *4*, 104003.

(9) Beekmann, U.; Zahel, P.; Karl, B.; Schmölz, L.; Börner, F.; Gerstmeier, J.; Werz, O.; Lorkowski, S.; Wiegand, C.; Fischer, D.; Kralisch, D. Modified Bacterial Cellulose Dressings to Treat Inflammatory Wounds. *Nanomaterials* **2020**, *10*, 2508.

(10) Qu, J.; Zhao, X.; Liang, Y.; Xu, Y.; Ma, P. X.; Guo, B. Degradable conductive injectable hydrogels as novel antibacterial, anti-oxidant wound dressings for wound healing. *Chem. Eng. J.* **2019**, *362*, 548−560.

(11) Wang, F.; Zhang, W.; Shao, Z.; Sun, Y.; Ru, C. Electrospinning system with tunable collector for fabricating three-dimensional nanofibrous structures. *Micro Nano Lett.* **2014**, *9*, 24−27.

(12) Wang, Z.; Lin, M.; Xie, Q.; Sun, H.; Huang, Y.; Zhang, D.; Yu, Z.; Bi, X.; Chen, J.; Wang, J.; Shi, W.; Gu, P.; Fan, X. Electrospun silk fibroin/poly(lactide-co-epsilon-caprolactone) nanofibrous scaffolds for bone regeneration. *Int. J. Nanomedicine* **2016**, *11*, 1483−1500.

(13) Masaeli, E.; Karamali, F.; Loghmani, S.; Eslaminejad, M. B.; Nasr-Esfahani, M. H. Bio-engineered electrospun nanofibrous membranes using cartilage extracellular matrix particles. *J. Mater. Chem. B* **2017**, *5*, 765−776.

(14) Souliotis, K.; Kalemikerakis, I.; Saridi, M.; Papageorgiou, M.; Kalokerinou, A. A cost and clinical effectiveness analysis among moist wound healing dressings versus traditional methods in home care patients with pressure ulcers. *Wound Repair Regen.* **2016**, *24*, 596−601.

(15) Schmidt, S. J.; Holt, B. D.; Arnold, A. M.; Sydlik, S. A. Polyester functional graphenic materials as a mechanically enhanced scaffold for tissue regeneration. *RSC Adv.* **2020**, *10*, 8548−8557.

(16) Augustine, R.; Rehman, S. R. U.; Ahmed, R.; Zahid, A. A.; Sharifi, M.; Falahati, M.; Hasan, A. Electrospun chitosan membranes containing bioactive and therapeutic agents for enhanced wound healing. *Int. J. Biol. Macromol.* **2020**, *156*, 153−170.

(17) Tang, Y.; Lan, X.; Liang, C.; Zhong, Z.; Xie, R.; Zhou, Y.; Miao, X.; Wang, H.; Wang, W. Honey loaded alginate/PVA nanofibrous membrane as potential bioactive wound dressing. *Carbohydr. Polym.* **2019**, *219*, 113−120.

(18) Mouro, C.; Fangueiro, R.; Gouveia, I. C. Preparation and Characterization of Electrospun Double-layered Nanocomposites Membranes as a Carrier for Centella asiatica (L.). *Polymer* **2020**, *12*, 2653.

(19) Pereira, R. F.; Bártolo, P. J. Traditional Therapies for Skin Wound Healing. *Adv. Wound Care* **2016**, *5*, 208−229.

(20) Janila, P.; Nigam, S. N.; Pandey, M. K.; Nagesh, P.; Varshney, R. K. Groundnut improvement: use of genetic and genomic tools. *Front. Plant Sci.* **2013**, *4*, 23.

(21) Rahman, S.; Carter, P.; Bhattarai, N. Aloe Vera for Tissue Engineering Applications. *J. Funct. Biomater.* **2017**, *8*, 6.

(22) Malviya, S.; Arvind; Jha, A.; Hettiarachchy, N. Antioxidant and antibacterial potential of pomegranate peel extracts. *J. Food Sci. Technol.* **2014**, *51*, 4132−4137.

(23) Barathikannan, K.; Venkatadri, B.; Khusro, A.; Al-Dhabi, N. A.; Agastian, P.; Arasu, M. V.; Choi, H. S.; Kim, Y. O. Chemical analysis of Punica granatum fruit peel and its in vitro and in vivo biological properties. *BMC Complement Altern. Med.* **2016**, *16*, 264.

(24) Mphahlele, R. R.; Fawole, O. A.; Makunga, N. P.; Opara, U. L. Effect of drying on the bioactive compounds, antioxidant, antibacterial and antityrosinase activities of pomegranate peel. *BMC Complement Altern. Med.* **2016**, *16*, 143.

(25) Mastrogiovanni, F.; Bernini, R.; Basiricò, L.; Bernabucci, U.; Campo, M.; Romani, A.; Santi, L.; Lacetera, N. Antioxidant and anti-

inflammatory effects of pomegranate peel extracts on bovine mammary epithelial cells BME-UV1. *Nat. Prod. Res.* **2020**, *34*, 1465−1469.
(26) Poor, H. M. H.; Hosseinzadeh, S.; Aminlari, M. Wound healing potential of pomegranate peel extract in human dermal fibroblasts through regulating the expression of FN1 gene. *S. Afr. J. Bot.* **2022**, *146*, 222−229.
(27) Zare, E. N.; Lakouraj, M. M.; Mohseni, M. Biodegradable polypyrrole/dextrin conductive nanocomposite: Synthesis, characterization, antioxidant and antibacterial activity. *Synth. Met.* **2014**, *187*, 9.
(28) Skrt, M.; Albreht, A.; Vovk, I.; Constantin, O. E.; Râpeanu, G.; Sežun, M.; Črnivec, I. G. O.; Zalar, U.; Ulrih, N. P. Extraction of Polyphenols and Valorization of Fibers from Istrian-Grown Pomegranate (Punica granatum L.). *Foods* **2022**, *11*, 2740.
(29) Kharchoufi, S.; Licciardello, F.; Siracusa, L.; Muratore, G.; Hamdi, M.; Restuccia, C. Antimicrobial and antioxidant features of 'Gabsi pomegranate peel extracts. *Ind. Crops Prod.* **2018**, *111*, 345−352.
(30) He, S.-W.; Li, S.-S.; Hu, Z.-M.; Yu, J.-R.; Chen, L.; Zhu, J. Effects of three parameters on the diameter of electrospun poly(ethylene oxide) nanofibers. *J. Nanosci. Nanotechnol.* **2011**, *11*, 1052−1059.
(31) Mahalakshmi, S.; Alagesan, T.; Parthasarathy, V.; Anbarasan, R. Thermal degradation and crystallization kinetics studies on synthesized calcium mercaptosuccinate end-capped poly(ε-caprolactone) nanocomposite. *Polym. Bull.* **2019**, *76*, 4991−5009.
(32) Ponjavic, M.; Nikolic, M. S.; Nikodinovic-Runic, J.; Ilic-Tomic, T.; Djonlagic, J. Controlled drug release carriers based on PCL/PEO/PCL block copolymers. *Int. J. Polym. Mater. Polym. Biomater.* **2019**, *68*, 308−318.
(33) Khosravi, A.; Ghasemi-Mobarakeh, L.; Mollahosseini, H.; Ajalloueian, F.; Rad, M. M.; Norouzi, M.; Jokandan, M. S.; Khoddami, A.; Chronakis, I. S. Immobilization of silk fibroin on the surface of PCL nanofibrous scaffolds for tissue engineering applications. *J. Appl. Polym. Sci.* **2018**, *135*, 46684.
(34) Alhusaiki-Alghamdi, H. M. The spectroscopic and physical properties of PMMA/PCL blend incorporated with graphene oxide. *Results Phys.* **2021**, *24*, No. 104125.
(35) Poornima, B.; Korrapati, P. S. Fabrication of chitosan-polycaprolactone composite nanofibrous scaffold for simultaneous delivery of ferulic acid and resveratrol. *Carbohydr. Polym.* **2017**, *157*, 1741−1749.
(36) Ben-Ali, S.; Akermi, A.; Mabrouk, M.; Ouederni, A. Optimization of extraction process and chemical characterization of pomegranate peel extract. *Chem. Pap.* **2018**, *72*, 2087−2100.
(37) He, Y.; Li, J.; Uyama, H.; Kobayashi, S.; Inoue, Y. Hydrogen-Bonding Interaction and Miscibility between Poly(ε-caprolactone) and Enzymatically Polymerized Novel Polyphenols. *J. Polym. Sci.* **2001**, *39*, 2898−2905.
(38) Arab, M.; Jallab, M.; Ghaffari, M.; Moghbelli, E.; Saeb, M. R. Synthesis, rheological characterization, and antibacterial activity of polyvinyl alcohol (PVA)/ zinc oxide nanoparticles wound dressing, achieved under electron beam irradiation. *Iran. Polym. J.* **2021**, *30*, 1019−1028.
(39) Rosa, M. D.; Carteni', M.; Petillo, O.; Calarco, A.; Margarucci, S.; Rosso, F.; Rosa, A. D.; Farina, E.; Grippo, P.; Peluso, G. Cationic polyelectrolyte hydrogel fosters fibroblast spreading, proliferation, and extracellular matrix production: Implications for tissue engineering. *J. Cell. Physiol.* **2004**, *198*, 133−143.
(40) Chan, C.; Gan, R.; Shah, N. P.; Corke, H. Enhancing antioxidant capacity of Lactobacillus acidophilus-fermented milk fortified with pomegranate peel extracts. *Food Biosci.* **2018**, *26*, 185.
(41) Kuo, S. W.; Huang, C. F.; Chang, F. C. Study of Hydrogen-Bonding Strength in Poly(ϵ-caprolactone) Blends by DSC and FTIR. *J. Polym. Sci.* **2001**, *39*, 1348.
(42) Jiang, S.; Song, P.; Guo, H.; Zhang, X.; Ren, Y.; Liu, H.; Song, X.; Kong, M. Blending PLLA/tannin-grafted PCL fiber membrane for skin tissue engineering. *J. Mater. Sci.* **2017**, *52*, 1617−1624.
(43) Magangana, T. P.; Makunga, N. P.; Fawole, O. A.; Opara, U. L. Effect of Solvent Extraction and Blanching Pre-Treatment on Phytochemical, Antioxidant Properties, Enzyme Inactivation and Antibacterial Activities of 'Wonderful' Pomegran ate Peel Extracts. *Processes* **2021**, *9*, 1012.
(44) Jiang, L.; Liu, T.; He, H.; Pham-Huy, L. A.; Li, L.; Pham-Huy, C.; Xiao, D. Adsorption behavior of pazufloxacin mesilate on amino-functionalized carbon nanotubes. *J. Nanosci. Nanotechnol.* **2012**, *12*, 7271−7279.
(45) Soybir, O. C.; Gürdal, S.; Oran, E.; Tülübaş, F.; Yüksel, M.; Akyıldız, A.; Bilir, A.; Soybir, G. R. Delayed cutaneous wound healing in aged rats compared to younger ones. *Int. Wound J.* **2012**, *9*, 478−487.
(46) Wu, X.; Venkitasamy, C.; McHugh, T.; Pan, Z. Process Development for Antioxidant Extraction from Wet Pomegranate Peel. *Trans. ASABE* **2021**, *64*, 191−202.
(47) Sharayei, P.; Azarpazhooh, E.; Zomorodi, S.; Ramaswamy, H. S. Ultrasound assisted extraction of bioactive compounds from pomegranate (Punica granatum L.) peel. *LWT Food Sci. Technol.* **2019**, *101*, 342−350.
(48) Davis, S. C.; Gil, J.; Solis, M.; Higa, A.; Mills, A.; Simms, C.; Pena, P. V.; Li, J.; Raut, V. Antimicrobial effectiveness of wound matrices containing native extracellular matrix with polyhexamethylene biguanide. *Int. Wound J.* **2022**, *19*, 86−99.
(49) Almagor, J.; Temkin, E.; Benenson, I.; Fallach, N.; Carmeli, Y.; on behalf of the DRIVE-AB consortium. The impact of antibiotic use on transmission of resistant bacteria in hospitals: Insights from an agent-based model. *PLoS One* **2018**, *13*, No. e0197111.
(50) Ismail, T.; Suleman, R.; Akram, K.; Hameed, A.; Llah, I.; Amir, M.; Akhtar, S. Pomegranate (Punica granatum L.) Peel Extracts Inhibit Microbial Growth and Lipid Oxidation in Minced Shrimps Stored at 4°C. *J. Aquat. Food Prod. Technol.* **2019**, *28*, 84−92.
(51) Tzeng, J.; Weng, C.; Yen, L.; Gaybullaev, G.; Chang, C.; Luna, M. D. G.; Lin, Y. Inactivation of pathogens by visible light photocatalysis with nitrogen-doped TiO2 and tourmaline-nitrogen co-doped TiO_2. *Sep. Purif. Technol.* **2021**, *274*, No. 118979.
(52) Tayel, A. A.; El-Tras, W. F. Anticandidal activity of pomegranate peel extract aerosol as an applicable sanitizing method. *Mycoses* **2010**, *53*, 117−122.
(53) Bae, J.-Y.; Seo, Y.-H.; Oh, S.-W. Antibacterial activities of polyphenols against foodborne pathogens and their application as antibacterial agents. *Food Sci. Biotechnol.* **2022**, *31*, 985−997.
(54) Wang, H.; Hao, L.; Wang, P.; Chen, M.; Jiang, S.; Jiang, S. Release kinetics and antibacterial activity of curcumin loaded zein fibers. *Food Hydrocoll.* **2017**, *63*, 437−446.
(55) Ozdemir, K. G.; Yilmaz, H.; Yilmaz, S. In vitro evaluation of cytotoxicity of soft lining materials on L929 cells by MTT assay. *J. Biomed. Mater. Res. B Appl. Biomater.* **2009**, *90*, 82−86.
(56) Ponnusamy, Y.; Chear, N. J.-Y.; Ramanathan, S.; Lai, C.-S. Polyphenols rich fraction of Dicranopteris linearis promotes fibroblast cell migration and proliferation in vitro. *J. Ethnopharmacol.* **2015**, *168*, 305−314.
(57) Chandika, P.; Ko, S.; Jung, W. Marine-derived biological macromolecule-based biomaterials for wound healing and skin tissue regeneration. *Int. J. Biol. Macromol.* **2015**, *77*, 24−35.

https://doi.org/10.1021/acsomega.2c08180
ACS Omega 2023, 8, 20323−20331